

Faculty of Engineering
Faculty of Engineering - Papers

University of Wollongong

Year 2007

Development and application of
constitutive model for railway ballast

B. Indraratna* W. Salim†
C. Rujikiatkamjorn‡

*University of Wollongong, indra@uow.edu.au

†University of Wollongong

‡University of Wollongong, cholacha@uow.edu.au

This paper was originally published as: Indraratna, B, Wadud, S & Rujikiatkamjorn, C, Development and application of constitutive model for railway ballast, in Yin, JH, Li, XS, Yeung, AT & Desai, CS (eds.), International Workshop on Constitutive Modelling, Hong Kong, January 2007, 685-696.

This paper is posted at Research Online.

<http://ro.uow.edu.au/engpapers/329>

DEVELOPMENT AND APPLICATION OF CONSTITUTIVE MODEL FOR RAILWAY BALLAST

Buddhima Indraratna¹, Wadud Salim² and Cholachat Rujikiatkamjorn²

Abstract: This *Discussion Paper* includes an elasto-plastic stress-strain constitutive model developed at the University of Wollongong, Australia, for coarse granular aggregates such as ballast, incorporating the degradation of particles as a particular feature. An attempt has also been made to extend the monotonic loading model to a cyclic stress-strain relationship. Most available constitutive models do not consider the breakage of particles during shearing, and the effects of cyclic loading on particle degradation and plastic deformation are rarely found in the literature. The developed model is based on the critical state framework and is able to predict the stress-strain and volume change behavior of coarse granular aggregates accurately. The model well captures the plastic dilation and contraction features under various confining pressures, and the strain-hardening and post-peak strain-softening behavior is adequately simulated.

INTRODUCTION

Various constitutive models for soils and aggregates have been proposed by several researchers in the past in order to simulate the monotonic loading response of these materials (e.g. Roscoe et al., 1963; Schofield and Wroth, 1968; Lade, 1977; Pender, 1978). A number of attempts were also made by the researchers to simulate the cyclic response of granular media. In the case of railway ballast, the progressive change in particle geometry due to internal attrition, grinding, splitting and crushing (i.e. degradation) under cyclic traffic loads further complicates the stress-strain relationship. The plastic deformation and particle degradation of coarse aggregates such as ballast under cyclic loading have not been simulated properly. In this paper, a constitutive model proposed by Salim and Indraratna (2004) and Indraratna and Salim (2005) will be discussed to some details including the required parameters, relevant laboratory testing and model validation. In this model, a non-associated flow and kinematic type of yield locus have been adopted, and a plastic flow rule incorporating the energy consumption due to particle breakage has been employed. The effects of particle breakage on the plastic distortional (deviatoric) and volumetric strains are incorporated in the model. The proposed monotonic loading model has been extended to simulate the response of coarse granular media under complex cyclic loading.

DEVELOPMENT OF THE MODEL

Modeling of Particle Breakage

Indraratna and Salim (2002) developed a relationship between the deviator stress ratio (q/p), rate of dilation ($d\varepsilon_v/d\varepsilon_l$), basic friction angle for granular aggregates (ϕ_j), and the rate of energy consumption due to particle breakage. For an axisymmetric specimen under triaxial compression (Fig. 1a), they have shown the following energy balance equation using the Mohr-Coulomb theory:

¹ Professor of Civil Engineering, Faculty of Engineering, University of Wollongong, Wollongong City, NSW 2522, Australia, E-mail: indra@uow.edu.au

² Research Fellow, Faculty of Engineering, University of Wollongong, Wollongong City, NSW 2522, Australia

$$\sigma'_1 \delta \varepsilon_1 - \sigma'_3 \delta \varepsilon_1 r_n \tan \beta_i = \sigma'_1 \delta \varepsilon_1 \tan \beta_i \tan \phi_\mu + \sigma'_3 \delta \varepsilon_1 r_n \tan \phi_\mu + \delta E_B \quad (1)$$

where, σ'_1 , σ'_3 are major and minor principal stresses, respectively, $\delta \varepsilon_1$ is finite increment of major principal strain, r_n is the ratio between the average number of contacts per unit length in the direction of minor and major principal stresses, β_i is angle of slip plane with the direction of major principal stress at contact i , ϕ_μ is interparticle friction angle between two particles and δE_B is incremental energy consumed due to particle breakage during shearing in a unit volume of aggregate.

Equation (1) can be rewritten in terms of mean effective stress (p') and deviatoric stress (q) as:

$$\frac{q}{p'} = \frac{r_n \tan(\beta_i + \phi_\mu) - 1}{\left[\frac{2}{3} + \frac{1}{3} r_n \tan(\beta_i + \phi_\mu) \right]} + \frac{\delta E_B}{p' \delta \varepsilon_1 \left[\frac{2}{3} + \frac{1}{3} r_n \tan(\beta_i + \phi_\mu) \right] [1 - \tan \beta_i \tan \phi_\mu]} \quad (2)$$

Rowe (1962) indicated that the interparticle friction angle (ϕ_μ) should be replaced by ϕ_f , which is the basic friction angle of aggregates after correction for dilatancy. The energy spent on the rearrangement of particles during shearing has been included in ϕ_f . Rowe didn't consider the breakage of particles during shearing, hence ϕ_f represents the basic friction angle of aggregates excluding dilatancy and particle breakage.

Using the minimum energy ratio principle, Ueng and Chen (2000) showed the following two expressions for the ratio r_n and the critical sliding angle β_c :

$$r_n = \frac{1 - \frac{d\varepsilon_v}{d\varepsilon_1}}{\tan \beta_c} \quad (3)$$

$$\beta_c = 45^\circ - \frac{\phi_f}{2} \quad (4)$$

where, $d\varepsilon_v$ is the volumetric strain increment (compression is taken as positive) of the triaxial specimen corresponding to $d\varepsilon_1$.

Indraratna and Salim (2002) indicated that the increment in energy consumption due to particle breakage may be related to the increment in breakage index as given by $dE_B = f(dB_g)$, where B_g is the particle breakage index (Marsal, 1967). Substituting Equations 3 and 4, ϕ_μ by ϕ_f and $\beta_i = \beta_c$ into Equation 2, and using the differential increment terms, the deviator stress ratio becomes (Indraratna and Salim, 2002):

$$\frac{q}{p'} = \frac{3(1 - d\varepsilon_v/d\varepsilon_1) \tan^2(45^\circ + \phi_f/2) - 3}{\left[2 + (1 - d\varepsilon_v/d\varepsilon_1) \tan^2(45^\circ + \phi_f/2) \right]} + \frac{3f(dB_g/d\varepsilon_1)(1 + \sin \phi_f)}{p' \left[2 + (1 - d\varepsilon_v/d\varepsilon_1) \tan^2(45^\circ + \phi_f/2) \right]} \quad (5)$$

where, $d\varepsilon_l$ and $d\varepsilon_v$ are the increments of major principal strain and volumetric strain, respectively. The parameter p' is the mean effective stress, q is the deviator stress and dB_g is the increment of breakage index associated with axial strain change $d\varepsilon_l$. The function $f(dB_g/d\varepsilon_l)$ in Equation (5) remains to be determined based on laboratory triaxial testing. Since this formulation employs the stress invariants, which include all normal and shear stresses in an

element, it can be applied to a conventional triaxial ($\sigma_2 = \sigma_3$) state as well as to a true triaxial state.

Contribution of Particle Breakage to Friction Angle

The peak friction angle (ϕ_p) of ballast can be calculated from the triaxial test results of peak principal stress ratio, as given in the following relationship:

$$\left(\frac{\sigma'_1}{\sigma'_3}\right)_p = \frac{1 + \sin \phi_p}{1 - \sin \phi_p} \quad (6)$$

Equation (6) provides an upper limit for the internal friction angle of aggregates. In contrast, the basic friction angle (ϕ_f) with no dilatancy and particle breakage provides a lower limit (Fig. 1b, Indraratna and Salim, 2002). It shows that the difference between ϕ_p and ϕ_f at low confinement is very high due to higher dilatancy. At low stresses, the degree of particle breakage is also low, and therefore, the difference between ϕ_{fb} and ϕ_f is also small, where ϕ_{fb} is the apparent friction angle including the contribution of particle breakage but excluding the effect of dilation. As confining pressure increases, the difference between ϕ_{fb} and ϕ_f increases, which is attributed to the higher rate of particle degradation (i.e. increased energy consumption for particle breakage). At very high confining pressure, a higher rate of particle breakage contributes to an increase in the friction angle; however, dilatancy becomes insignificant, and volumetric contraction adversely affects the friction angle. The peak friction angle (ϕ_p) computed from the laboratory triaxial test results can be viewed as the combination of basic friction angle ϕ_f , and the effects of dilatancy and particle breakage.

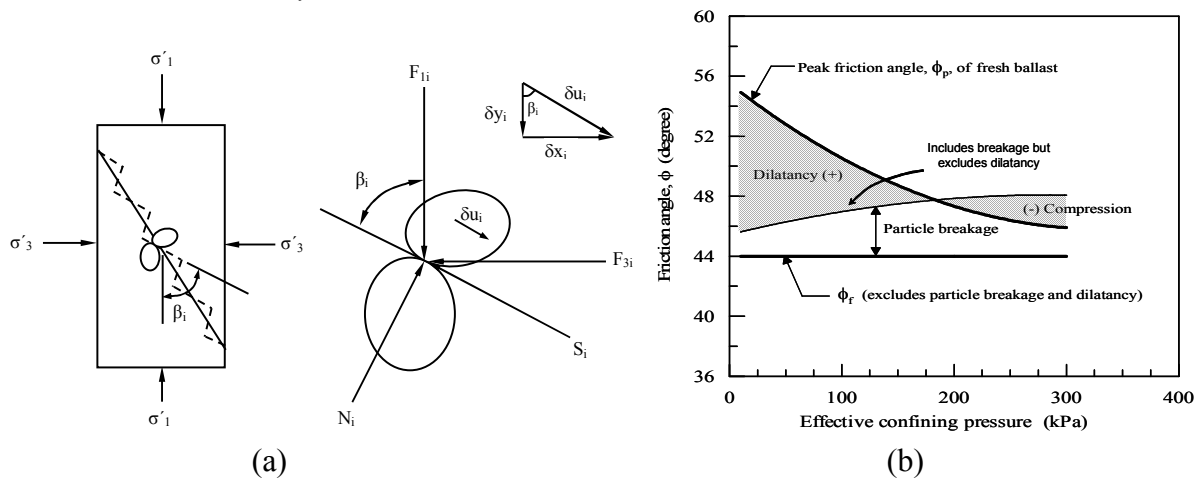


Figure 1 (a) Triaxial compression of ballast and details of contact forces and deformations of two particles at contact, (b) Effect of particle breakage and dilatancy on friction angle (after Indraratna and Salim, 2002, Indraratna and Salim, 2005)

Indraratna et al. (2005) conducted a series of cyclic triaxial tests using a large-scale triaxial apparatus to investigate the effects of confining pressure on ballast degradation. They introduced a new Ballast Breakage Index (BBI, Fig. 2a) to quantify the breakage characteristics of ballast as given below (Indraratna et al., 2005):

$$BBI = A / (A + B) \quad (7)$$

where, A is the area between the initial particle size distribution (before test) and final particle size distribution (after the test), and B is the potential breakage or the area between the arbitrary boundary of maximum breakage and the final particle size distribution (Fig. 2a).

Figure 2b shows the effects of confining pressure on particle degradation. The results of ballast breakage have been divided into three regions namely: (I) dilatant unstable, (II) optimum and (III) compressive stable degradation zones (Indraratna et al., 2005). At low confining pressure of region (I) where $\sigma_3' < 30$ kPa, ballast specimens are subjected to rapid and considerable axial and expansive radial strains. This leads to an overall volumetric increase or dilation. As the confining pressure is increased to the optimum region ($\sigma_3' = 30-75$ kPa), particles are held together in an optimum array with sufficient lateral confinement so as to provide an optimum contact stress distribution and increased inter-particle contact areas. This leads to the reduction of the risk of breakage associated with stress concentrations. As σ_3' is further increased to the compressive stable region ($\sigma_3' > 75$ kPa), particles fail not only at the beginning of loading when the axial strain rates are the greatest, but also by the process of fatigue as the number of cycles increases.

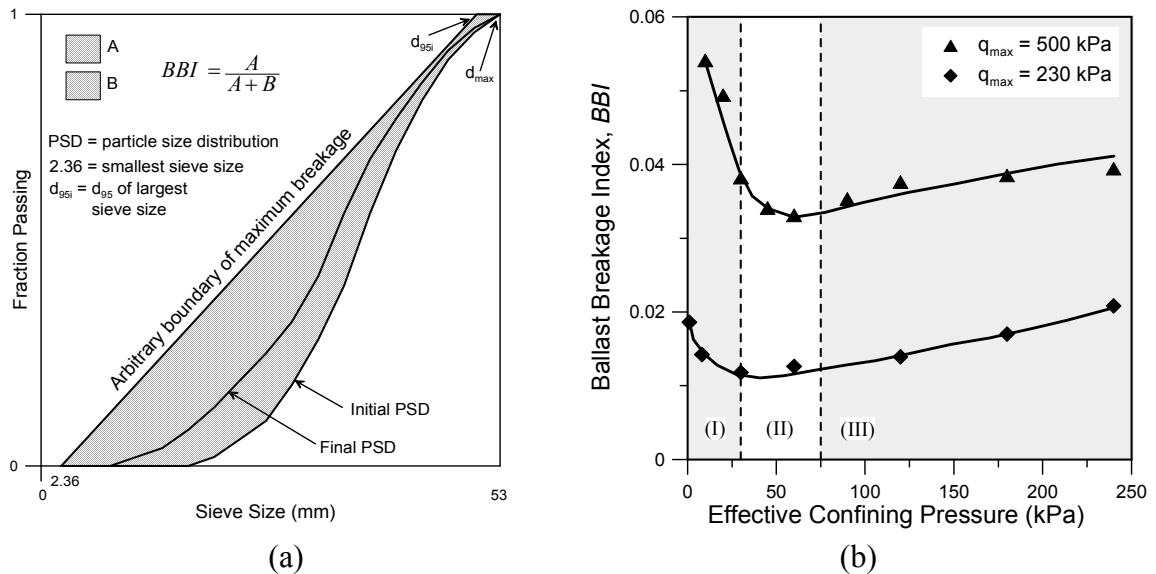


Figure 2 (a) Evaluation of the Ballast Breakage Index BBI (b) Effect of confining pressure on ballast degradation under cyclic loading (Indraratna et al. 2005)

Constitutive Modeling for Monotonic Loading

Main assumptions for developing the yield and hardening functions are as follows (Salim and Indraratna, 2004):

Coarse granular aggregates experience plastic strains, when there is a change in stress ratio, q/p ($= \eta$). The yield loci are represented by constant stress ratio ($\eta = \text{constant}$) lines in the p - q plane (Fig. 3a). The yield function f , specifying the yield locus for the current stress

ratio η_j , is expressed by Pender (1978) as:

$$f = q - \eta_j p = 0 \quad (8)$$

Figure 3b shows the directions of plastic strain increments for different yield loci. Each plastic strain increment vector has a volumetric component associated with its deviatoric (distortional) component.

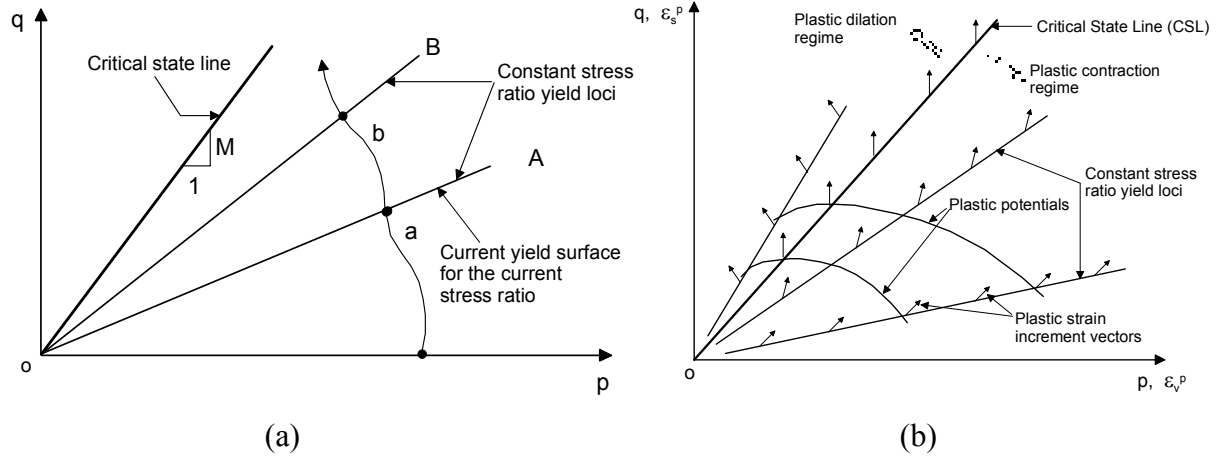


Figure 3 (a) Yield loci represented by constant stress ratio lines in p - q plane and (b) Plastic strain increment vectors and plastic potentials (Salim and Indraratna, 2004, Indraratna and Salim, 2005)

The undrained stress paths are parabolic in the p - q plane, and are expressed by the following relationship (Pender 1978):

$$(\eta/M)^2 = (p_{cs}/p)((1 - p_o/p)/(1 - p_o/p_{cs})) \quad (9)$$

where, p_{cs} is the value of p on the critical state line at the current void ratio, and p_o is the value of p at the intersection of the initial stress ratio line with an imaginary undrained stress path which passes through the current stress (p, q) point and current (p_{cs}, Mp_{cs}) point corresponding to the current void ratio. M is the critical state friction ratio for granular material.

The partial derivatives of the plastic potential g with respect to p and q can be expressed by:

$$\frac{\partial g}{\partial q} = 1 \quad (10)$$

$$\frac{\partial g}{\partial p} = \frac{9(Mp - q) + B\{\chi + \mu(M - q/p_{cs})\}}{(9 + 3M)p - 2qM} = \frac{9(M - \eta) + (B/p)\{\chi + \mu(M - \eta^*)\}}{9 + 3M - 2\eta M} \quad (11)$$

$$\text{and } B = \beta \left[\frac{(9 - 3M)(6 + 4M)}{6 + M} \right] / \ln \left(\frac{p_{cs(i)}}{p_{(i)}} \right) = \text{constant} \quad (11a)$$

where, χ and μ are the material constants defining the rate of particle breakage, β is the constant of proportionality between the rate of energy consumption due to particle breakage and the rate of particle breakage, $\eta^* = \eta(p/p_{cs})$, and the subscript (i) indicates the initial value.

The hardening function h is given by:

$$h = \frac{2\kappa(p_o/p_{cs} - 1)(9 + 3M - 2\eta M)\eta}{M^2(1 + e_i)(2p_o/p - 1)p_{cs}[9(M - \eta) + (B/p)\{\chi + \mu(M - \eta^*)\}]} \quad (12)$$

where, e_i = initial void ratio and κ is the elastic swelling/recompression constant.

The ratio between plastic volumetric strain increment $d\varepsilon_v^p$ and plastic distortional strain increment $d\varepsilon_s^p$ for a drained test may be expressed as follows:

$$\frac{d\varepsilon_v^p}{d\varepsilon_s^p} = \frac{9(M - \eta)}{9 + 3M - 2\eta^* M} + \left(\frac{B}{p}\right) \left[\frac{\chi + \mu(M - \eta^*)}{9 + 3M - 2\eta^* M}\right] \quad (13)$$

For a strain-controlled condition (e.g. laboratory test), the stress ratio increment is given by (Indraratna and Salim, 2005):

$$d\eta = \frac{M^2(1 + e_i)(2p_o/p - 1)[9(M - \eta^*) + (B/p)\{\chi + \mu(M - \eta^*)\}]d\varepsilon_s^p}{2\alpha\kappa(p/p_{cs})(1 - p_{o(i)}/p_{cs(i)})(9 + 3M - 2\eta^* M)\eta} \quad (14)$$

The elastic strain increments can be easily modeled using the theory of elasticity employing the elastic constants G and κ , where G is the elastic shear modulus.

If the particle breakage during shearing is ignored, Equation 5 at the critical state (i.e. $dp' = dq = d\varepsilon_v = 0$ and $\phi_f = \phi_{cs}$) is reduced to the well-known critical state equation (Schofield and Wroth, 1968).

$$\left(\frac{q}{p'}\right)_{cs} = \frac{\tan^2(45^\circ + \phi_{cs}/2) - 1}{2/3 + 1/3 \times \tan^2(45^\circ + \phi_{cs}/2)} = \frac{6\text{Sin}\phi_{cs}}{3 - \text{Sin}\phi_{cs}} = M \quad (15)$$

Determination of Model Parameters

The parameters used in the above model can be evaluated using large-scale drained triaxial tests with the measurement of particle breakage, as summarized in Table 1 below. The parameters M and κ are similar to the critical state parameters predominantly based on the friction angle ϕ_{cs} (Schofield and Wroth, 1968). In order to study the behavior of ballast, two types of large-scale apparatus (i.e. large-scale triaxial apparatus and large prismatic triaxial apparatus) have been designed and built at the University of Wollongong (Fig. 4). The large-scale triaxial apparatus (Fig. 4a) can accommodate specimens of 300 mm diameter and 600 mm high, whereas the large prismatic triaxial rig (Fig. 4b) can accommodate specimens of 800 mm long, 600 mm wide, and 600 mm high. The latter one is a true triaxial apparatus where three independent principal stresses can be applied in the three mutually orthogonal directions.

Table 1 Model parameters

No.	Parameters (Symbol)	Evaluation approach	Required laboratory testing
1	M, G and κ	A series of drained triaxial compression tests at various effective confining pressures	Large-scale triaxial testing
2	Particle breakage index (B_g)	Refer to Marsal (1967)	Large-scale triaxial testing
3	Ballast Breakage Index BBI	Refer to Indraratna et al. (2005a)	Large-scale triaxial testing
4	β	Curve fitting (the slope of the plot of $dE_B/d\varepsilon_1$ versus $dB_g/d\varepsilon_1$, Fig. 5a)	Large-scale triaxial testing
5	χ and μ	Curve fitting by plotting the rate of particle breakage in terms of $\ln\{p_{cs(i)}/p(i)\} dB_g/d\varepsilon_s^p$ versus $(M - \eta^*)$ (Fig. 5b)	Large-scale triaxial testing
6	α	Match the initial stiffness of model predictions with experimental results	Large-scale triaxial testing

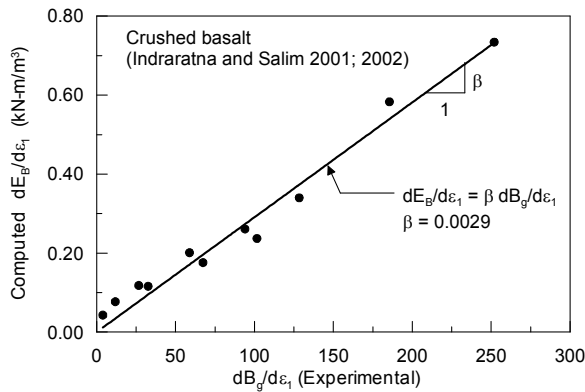


(a)

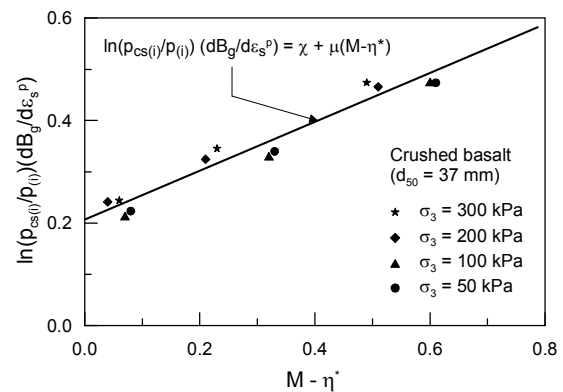


(b)

Figure 4 Large-scale triaxial apparatus built at the University of Wollongong, (a) large-scale triaxial apparatus and (b) Large prismoidal triaxial apparatus (Indraratna et al. 1998)
The model parameters β , χ and μ can be determined using the breakage measurements and other experimental results, as shown in Fig. 5.



(a)



(b)

Figure 5 (a) Relationship between the rate of energy consumption and rate of particle breakage and (b) Modeling of rate of particle breakage during triaxial shearing (Salim and Indraratna, 2004, Indraratna and Salim, 2005)

MODEL VALIDATION

Analytical and Finite Element Approach

In order to validate the model, both analytical and FEM predictions were made and compared with the experimental data (Indraratna and Salim, 2005). In predicting ballast response under monotonic loading using the analytical approach, the following model parameters were used: $M = 1.9$, $\kappa = 0.007$, $G = 80$ MPa, $\alpha = 28$, $\beta = 0.0029$ kN-m/m³, $\chi = 0.21$ and $\mu = 0.50$. In the finite element approach, the computer code ABAQUS has been employed to simulate the behavior of a cylindrical ballast specimen under triaxial loading. In

ABAQUS, the extended Drucker-Prager model with hardening was used to predict inelastic deformation of granular materials (Hibbit, Karlsson and Sorensen, Inc., 2002). Figure 6 shows the FEM stress-strain and volume change predictions compared with the analytical predictions and experimental results.

Both the analytical and FEM models predict the stress-strain response of ballast fairly well, but the proposed constitutive model incorporating ballast degradation is slightly better. Figure 6b clearly shows that the FEM model could not simulate the volumetric response of ballast well at high confining pressures (e.g. 200 and 300 kPa). This is because particle breakage, which is absent in ABAQUS model, becomes increasingly more significant at high stresses, hence, the subsequent overall contraction of the specimen is inevitable. The proposed constitutive model takes into account the breakage of particles and therefore, well simulates the volumetric response at higher confinement.

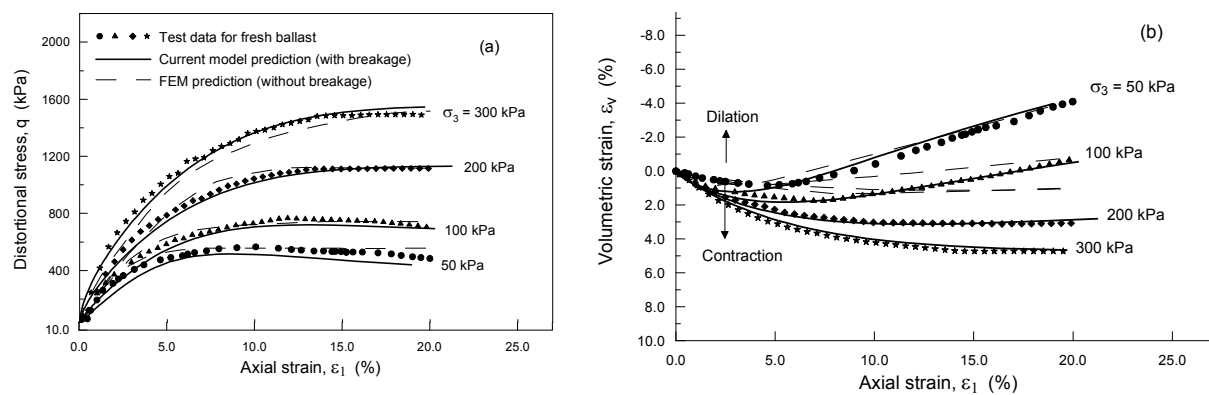


Figure 6 Experimental data of ballast compared with FEM analysis results and analytical model predictions, (a) stress-strain, and (b) volume change behaviour (Indraratna and Salim, 2005)

CONSTITUTIVE MODELING FOR CYCLIC LOADING: FURTHER EXTENSION

The classical theory of plasticity is unable to simulate the accumulation of plastic strains with increasing load cycles. To overcome this limitation, a new concept of bounding surface plasticity incorporating varying hardening function was proposed by Dafalias and Herrmann (1982) to simulate the response of geomaterials under cyclic loading. Similar concept has been employed by Indraratna and Salim (2005) to simulate the response of ballast under cyclic loading. Figure 7 illustrates the concept of bounding surface for a simple loading-unloading and reloading path 'a-b-c-d'. The constant stress ratio lines (OA, OB, OC, OD etc.) represent yield loci whereas the dotted curves are possible caps of the yield loci at very high stress levels. It is anticipated that at very high stress levels, ballast will yield in both isotropic compression ($\eta = 0$) and shearing (i.e. $d|\eta| > 0$), and that the degree of particle breakage will be very high at those stresses.

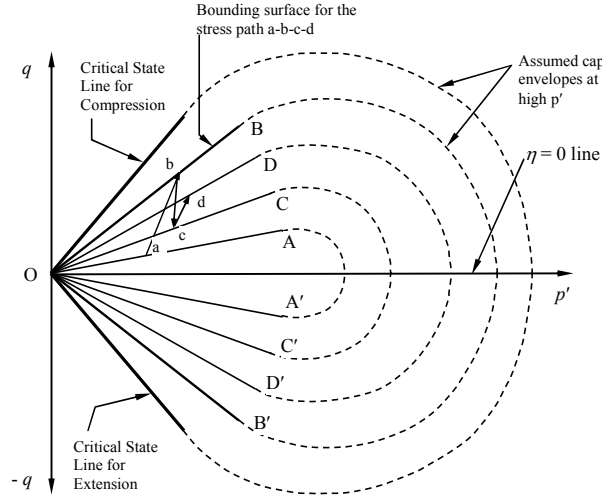


Figure 7 Bounding surface for a simplified stress path 'a-b-c-d' under cyclic loading (Salim, 2004; Indraratna and Salim, 2005)

If the stress ratio at point 'a' at the start of the loading path represents the maximum past stress ratio of ballast, then the line OA forms its current bounding surface. It is assumed that if the stress state is on the current bounding surface and the change of stress is directed towards the exterior of the bounding surface (i.e. away from the $\eta = 0$ line, or $d|\eta| > 0$), it represents 'loading', which causes plastic deformation, in addition to elastic strain. The plastic deformation associated with this 'loading' will be governed by the modified hardening function h , which is given by:

$$h = \frac{2\alpha\kappa(1/p_{cs})(1 - p_{o(i)}/p_{cs(i)})(9 + 3M - 2\eta^* M)(\eta - \eta_i)}{(M - \eta_i)^2(1 + e_i)(2p_o/p - 1)[9(M - \eta^*) + (B/p)\{\chi + \mu(M - \eta^*)\}]} \quad (16)$$

It is noted that a cyclic loading may commence from an initial stress ratio, η_i . The initial hardening function $h_{int(i)}$ and the evolution of plastic hardening function h_{int} , within the bounding surface are given by (Indraratna and Salim, 2005):

$$h_{int(i)} = h_i e^{-\xi_1 \varepsilon_v^p} \quad (17)$$

$$h_{int} = h_{int(i)} + (h_{bound} - h_{int(i)})R^\gamma e^{-\xi_2 \varepsilon_v^p} \quad (18)$$

$$R = (\eta - \eta_i) / (\eta_{bound} - \eta_i) \quad (19)$$

where, h_i = initial hardening function at the start of cyclic loading (e.g. $h_i = h$ at point 'a' in Fig. 7), h_{int} = hardening function at the interior of bounding surface (for 'reloading'), $h_{int(i)}$ = initial value of h_{int} for 'reloading', ξ_1 , ξ_2 and γ are dimensionless parameters, and the first two are related to cyclic hardening.

The function h_{int} for the first 'reloading' is modeled by Equation 18. For the second and subsequent 'reloadings', h_{int} is given by:

$$h_{int} = h_{int(i)} + (h_{bound} - h_{int(i)})R^\gamma e^{-\xi_3 \varepsilon_{v1}^p} \quad (20)$$

where, ξ_3 is another dimensionless parameter related to cyclic hardening, and ε_{v1}^p is the accumulated plastic volumetric strain since the end of the first load cycle.

APPLICATION TO CASE HISTORY

In the coastal areas of Australia, the rail tracks are constructed on embankments overlying soft and compressible formation soils. The passage of heavy haul trains with considerable imposed train loads over these soft deposits causes excessive track settlement and significant reduction in the load bearing capacity of the track. Indraratna et al. (2006) analyzed a railway track section using plane strain finite element model (PLAXIS) (Fig. 8a) to investigate the effects of geosynthetics and prefabricated vertical drains (PVDs) in the Northern New South Wales region. Table 2 summarises the soil properties used in the analysis. The predicted ballast settlements are plotted against the depth of geogrid placement, as shown in Fig. 8b. The analysis results indicate that the optimum location of geosynthetics in the ballast layer would be at 200mm depth. It was shown that when subgrade stiffness decreases, the sleeper deflection increases dramatically, which indicates that maintenance would be a crucial issue for tracks on soft formations. Figure 9a clearly shows that PVDs speed up the excess pore pressure dissipation. More than 65% excess pore pressure dissipates within the first 4-5 months. Figure 9b indicates that the lateral displacement of PVD stabilised soil underlying the compacted ballast is significantly reduced, especially at the shallower depth (< 2 m). This numerical example demonstrates the benefits of using short PVDs in soft formation soils beneath the rail tracks.

Table 2 Assumed parameters for soft soil foundation and ballasted track (300mm of ballast thickness and 1m thick compacted fill and crusted layer, Indraratna et al., 2006)

Depth of layer (m)	Material	c (kPa)	ϕ (degree)	$\lambda/(1+e_0)$	$\kappa/(1+e_0)$
+0.3	Ballast	-	45	-	-
0-1	Crust	29	29	-	-
1-10	Soft clay	10	25	0.15	0.03
10-30	Soft clay	15	20	0.12	0.02

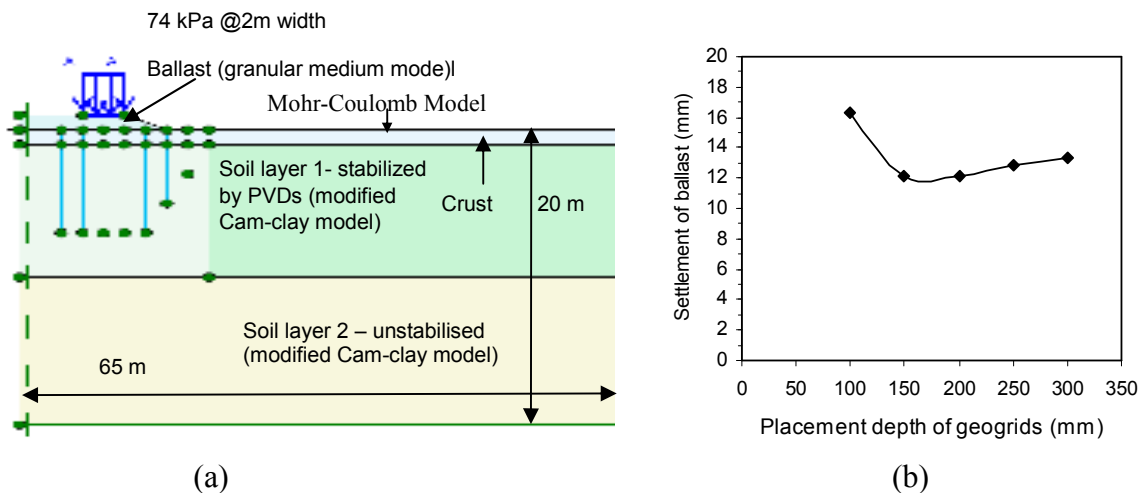


Figure 8 (a) Vertical cross section of track and formation (b) Optimum location of geosynthetics by the finite elements (Indraratna et al., 2006)

CONCLUSIONS

A new elasto-plastic stress-strain constitutive model incorporating particle breakage has been developed to simulate the behavior of coarse granular aggregates subjected to shearing. The model is based on the critical state concept, and employs a non-associated flow and a kinematic type yield locus (constant stress ratio). A plastic flow rule has been formulated incorporating particle breakage. Large-scale triaxial test results were used to calibrate the model parameters and also to validate the constitutive model. The numerical results clearly show that the current model accurately predicts the stress-strain and volume change behavior of ballast, particularly particle breakage under monotonic loading. This model has been extended to capture the cyclic behavior of ballast, and a further advancement of the model is ongoing at the University of Wollongong.

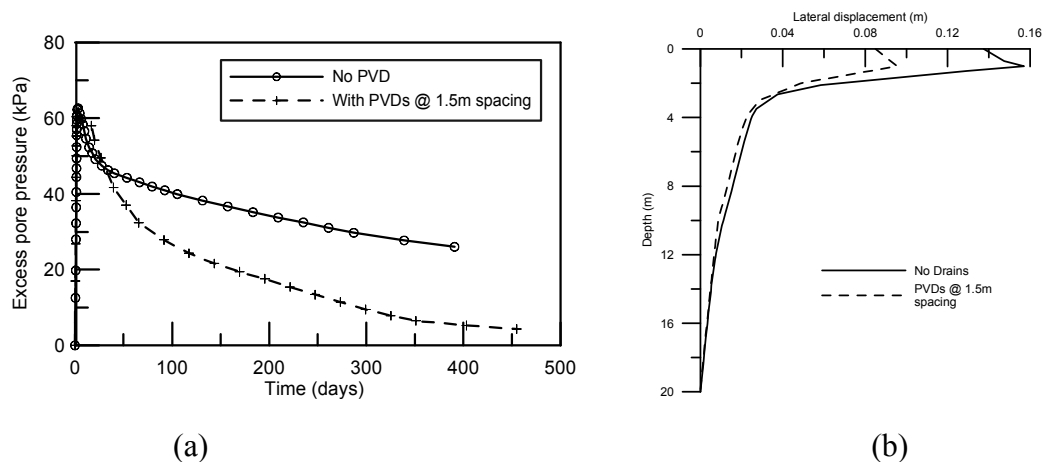


Figure 9 (a) Excess pore pressure dissipation at 2 m depth at centre line of loading strip and (b) Lateral displacement profiles near the embankment toe (Indraratna et al., 2006)

ACKNOWLEDGEMENTS

The authors are grateful for kind copyright permission to reproduce Figures, Tables and selected technical discussions from Canadian Geotechnical Journal, Geotechnique, and *Geotechnical Engineering*, Proc. of the Institution of Civil Engineers (UK). A number of current and past PhD students, namely, Dr. D. Ionescu and Dr. J. Lackenby have also contributed to the contents of this paper.

REFERENCES

- Dafalias, Y. F. and Herrmann, L. R. (1982). Bounding surface formulation of soil plasticity. In: Soil Mechanics - Transient and Cyclic Loads (edited by Pande and Zienkiewicz), 253-282.
- Hibbit, Karlsson and Sorensen, Inc. (2002). ABAQUS/Standard User's Manual. Version 6.3, Vol. 2.
- Indraratna, B. and Salim, W. (2002). Modelling of Particle Breakage of Coarse Aggregates Incorporating Strength and Dilatancy. Geotechnical Engineering, Proceedings of Inst. of Civil Engineers, UK, 155(4), 243-252.

- Indraratna, B. and Salim, W. (2005). _ Mechanics of Ballasted Rail Tracks - A Geotechnical Perspective, Taylor and Francis (UK), 237p
- Indraratna, B. and Ionescu, D and Christie, D. (1998). Shear Behavior of Railway Ballast based on Large Scale Triaxial Testing, Journal of Geotechnical and Geoenvironmental Engineering, ASCE, Vol. 124(5): 439-449.
- Indraratna, B., Lackenby, J. and Christie, D. (2005). Effect of confining pressure on the degradation of ballast under cyclic loading. Geotechnique, Institution of Civil Engineers, UK, 55(4): 325-328.
- Indraratna, B., Rujikiatkamjorn, C., Wijeyakulasuriya, V., Shahin, M. A. and Christie, D. (2006). Soft soil stabilization with special reference to railway embankments. Keynote Paper: 4th International Conference of Soft Soil Engineering, Vancouver, Canada, to be held in October.
- Lade, P. V. (1977). Elasto-plastic stress-strain theory for cohesionless soil with curved yield surfaces. International Journal of Solids and Structures, Vol. 13, pp. 1019-1035.
- Marsal, R. J. 1967. Large scale testing of rockfill materials. Journal of the Soil Mechanics and Foundations Division, ASCE, 93(SM2): 27-43.
- Pender, M. J. (1978). A model for the behavior of overconsolidated soil. Geotechnique, 28(1): 1-25.
- Roscoe, K.H., Schofield, A.N. and Wroth, C.P. (1958). On yielding of soils. Geotechnique, 8(1): 22-53.
- Rowe P. W. (1962). The stress-dilatancy relation for the static equilibrium of an assembly of particles in contact. Proceedings Royal Society, Vol. A269, pp. 500-527.
- Salim, M. W. (2004). The deformation and degradation aspects of ballast and constitutive modeling under cyclic loading. PhD thesis, University of Wollongong, Australia.
- Salim, W. and Indraratna, B. (2004). A New Elasto-plastic Constitutive Model For Granular Aggregates Incorporating Particle Breakage, Canadian Geotechnical Journal, 41: 657-671.
- Schofield, A.N. and Wroth, C.P. (1968). Critical State Soil Mechanics. McGraw Hill.
- Ueng, T. S. and Chen, T. J. (2000). Energy aspects of particle breakage in drained shear of sands. Geotechnique, Vol. 50, No. 1, pp. 65-72.